

Biological applications of high aspect ratio nanoparticles

Laura Ann Bauer, Nira S. Birenbaum and Gerald J. Meyer*

Departments of Chemistry and Materials Science and Engineering, Johns Hopkins University, 3400 N. Charles Street, Baltimore, MD 21218, USA

Received 13th October 2003, Accepted 11th November 2003

First published as an Advance Article on the web 14th January 2004

This review describes recent advances in nanomaterials fabrication that have led to the synthesis of high aspect ratio particles on nanometer length scales. The elongated structure of these materials often result in inherent chemical, electrical, magnetic, and optical anisotropy that can be exploited for interactions with cells and biomolecules in fundamentally new ways. We briefly describe the synthetic procedures that have been developed to fabricate nanorods, nanowires, and nanotubes. We summarize literature reports that describe the use of high aspect ratio nanoparticles for biological sensing, separations, and gene delivery. We emphasize the recent discovery of single nanowire field-effect transistors that may revolutionize biological sensing and yield extremely low detection limits. Separations technology with chemically modifiable nanotube membranes and with magnetic nanowires that can be tailored to selectively interact with molecules of interest is also described. Other areas of biotechnology that have been improved by the integration of high aspect ratio nanoparticles are also described.

technology. The nanometer size scale is particularly relevant in biology, because the dimensions of large biomolecules such as proteins and DNA, as well as those of many important sub-cellular structures, fall in the 1–1000 nm range. Historically, nanostructured materials were largely restricted to spherical particles of gold and silver. More recently, a wider variety of nanomaterials has been synthesized and used for biological applications. For example, commercially available spherical magnetic beads are used for cell separations,^{1,2} quantum dots have found use for long-term fluorescence assays in cells,³ and colloidal gold has been used for gene therapy.⁴ More complex particles can lead to new possibilities for unique interactions with biological molecules. Recent advances in nanomaterials fabrication have led to the synthesis of high aspect ratio particles on nanometer length scales. Because of their elongated structure, these materials often have inherent chemical, electrical, magnetic, and optical anisotropy, and they can interact with cells and biomolecules in fundamentally new ways. This is the subject of this review.

The review is organized as follows. We begin by describing the materials processing techniques used to fabricate high aspect ratio nanoparticles. We pay particular attention to materials that have already found biotechnological applications. We then discuss methods by which the particles can be chemically modified with appropriate agents for biological interactions. This section is followed by a review of the

I. Introduction

The integration of biology and materials at the nanoscale has the potential to revolutionize many fields of science and

Laura Ann Bauer was born in Orange, California. She received a B.S. degree in chemistry at the University of California at Berkeley. She is currently a graduate student at Johns Hopkins University under the supervision of Gerald J. Meyer.



Laura Ann Bauer

Nira S. Birenbaum was raised in Cleveland, Ohio. She received a B.S. degree in chemistry at the University of Rochester.



Nira S. Birenbaum

She is currently a graduate student at Johns Hopkins University under the supervision of Gerald J. Meyer.

Gerald J. Meyer was born in Oconomowoc Wisconsin in 1962. He received a B.S. degree in chemistry and mathematics at the State University of New York at Albany and a Ph.D. in chemistry from the University of Wisconsin at Madison under

the supervision of Professor Arthur B. Ellis. He undertook a postdoctoral position with Professor Thomas J. Meyer at the University of North Carolina at Chapel Hill before starting a faculty position at Johns Hopkins University where he is now a Professor of Chemistry. His principle research interests are in the applications of nanomaterials to solar energy conversion, environmental chemistry, and biotechnology.



Gerald J. Meyer

interesting new applications of these materials in biology, including separations technology, sensing, and gene delivery. The review concludes with a brief summary and a look forward to this exciting new interdisciplinary scientific area.

II. Synthesis of high aspect ratio nanoparticles

The many types of high aspect ratio nanoparticles are briefly summarized in Table 1.

Nanoporous membrane templated fabrication

The templated fabrication of nanowires was first realized by Possin in the late 1960s.⁵ In this approach, a membrane with uniform, nanometer diameter, cylindrical pores acts as a template. When material is deposited into the cylindrical pores of the membrane, it adopts their shape. If the template is dissolved, the material can retain the high aspect ratio of the pores, yielding wires with nanometer diameters.

Two types of templates are most often used for this approach: track-etch polycarbonate and anodized alumina. Alumina templates, made from a thin sheet of anodized aluminium, are readily commercially available in a variety of pore sizes or can be synthesized in the laboratory from aluminium foil (Fig. 1B).⁶ Polycarbonate templates are commercially available in a variety of pore sizes.⁷ Templates with diamond shaped pores, fabricated from nuclear track etching of mica, have also been reported.⁸

A general procedure for electrodeposition of conductive nanowires is as follows. A metallic under layer is sputter deposited onto one side of a membrane. An ohmic contact is made and this layer acts as the working electrode in a standard three-electrode electrochemical cell. An electrodeposition solution that contains a precursor of the material to be deposited is placed in the pores. The deposition is initiated with an applied potential. As material is electrodeposited, the nanowires "grow" from the bottom. A current vs. time plot is shown in Scheme 1.⁹ Region I corresponds to the deposition of materials into the pores of the membrane. As the material grows out of the pores, hemisphere caps grow on the ends of the nanowires (Region II), which then coalesce into a contiguous surface over the nanowires (Region III). By stopping the growth somewhere within Region I, nanowires are grown. Nickel,⁹ cobalt,⁹ gold,¹⁰ platinum,¹¹ silver,¹² ZnO,¹³ and other types of materials¹² have all been fabricated by the templated nanowire electrodeposition technique. Chien and co-workers examined the giant ferromagnetic properties of arrays of cobalt and nickel nanowires.⁹ An advantage of the templated electrodeposition of nanowires is the ability to make nanowires with segments of different materials. This can be achieved by altering the applied potential of a solution with more than one precursor, or by changing the deposition solution. For example, Natan and co-workers made sub-micrometer metallic barcodes by alternating Au and Ag segments along the length of a nanowire.¹⁴ For sensing and nanoelectrode applications, the nanowires can remain in the template and function as an array. For single-nanowire applications, removing the under layer and dissolving the template produces individual nanowires that can be isolated.

The templates can also be used to synthesize nanowires through chemical means. For example, sol-gel metal alkoxide precursors can be introduced into the pores and gelation can be initiated. Drying, in some cases at high temperatures, produces high aspect ratio metal oxide nanoparticles such as ZnO and TiO₂. Xu and co-workers have synthesized TiO₂ nanowires *via* an electrochemically induced sol-gel method (Scheme 2).¹⁵ They immersed an alumina membrane in a titania alkoxide solution and electrochemically induced sol formation within the membrane pores. They then annealed the

Table 1 Types of high aspect ratio nanoparticles

Type of nanoparticle	Materials	Synthetic method	Dimensions: diameter, length	Aspect ratio	Ref.
Nanowire	Ni, Au, Pt, Ag, Co, Cu, ZnO, conductive polymers, more	Templated electrodeposition	$d = 10\text{--}350\text{ nm}$, $l = \text{up to } 50\text{ }\mu\text{m}$	up to 250	5, 9, 10, 11, 12, 13
	TiO ₂ , ZnO	Sol-gel	$d = 10\text{--}350\text{ nm}$, $l = \text{up to } 50\text{ }\mu\text{m}$	250	15
	Silicon	Nanocluster-mediated vapor-liquid-solid growth	$d = 10\text{ nm}$, $l = > 1\text{ }\mu\text{m}$	> 100	37, 38
	MoO ₃ , Fe ₂ O ₃ , Cu ₂ O, Pd ¹⁰⁸	Electrodeposition on graphite surface	$d = 13\text{ nm}$ and up, $l = \text{microns}$	> 100	22
Nanotube	Cu, Au, and Ag	Electrodeposition on graphite surface	$d = 50\text{ nm}$, $l = \text{microns}$	> 20	22
	Gold	Templated electrodeless deposition	$d = 10\text{--}350\text{ nm}$, $l = \text{up to } 50\text{ }\mu\text{m}$	250	16, 17
	Silica	Sol-gel	$d = 10\text{--}350\text{ nm}$, $l = \text{up to } 50\text{ }\mu\text{m}$	250	18
	Carbon	High temperature: laser ablation, arc discharge, others	$d = 1.2\text{--}1.4\text{ nm}$, $l = \text{microns}$	> 100	33, 34, 35, 36
Nanorod	Gold	Surfactant mediated synthesis	$d = 20\text{ nm}$, $l = 400\text{ nm}$ in high yields, $2\text{ }\mu\text{m}$ in low yields	~ 20 in high yields, up to 100 in low yields	23, 24, 25
	CdSe	Surfactant mediated synthesis	$d = 3.3\text{--}5.0\text{ nm}$, $l = 18\text{--}36\text{ nm}$	2 to 10	26, 27, 28
	Cu	Micellar growth	$d = 6.6\text{--}13.4\text{ nm}$, $l = 12.0\text{--}25\text{ nm}$	1.7 to 3.7	30
	Se	Crystal growth	$d = 10\text{--}30\text{ nm}$, $l = \text{microns}$	> 100	29

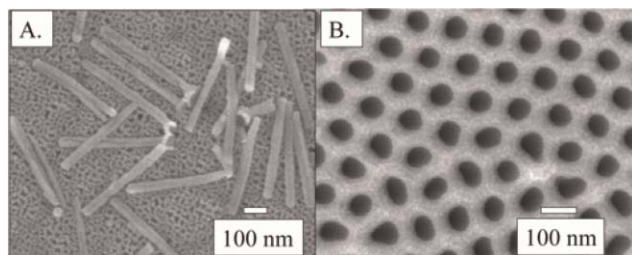
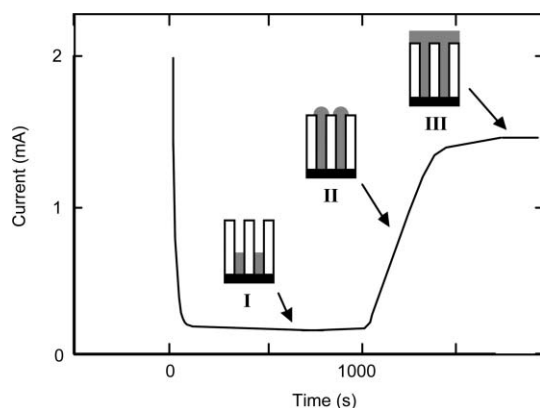


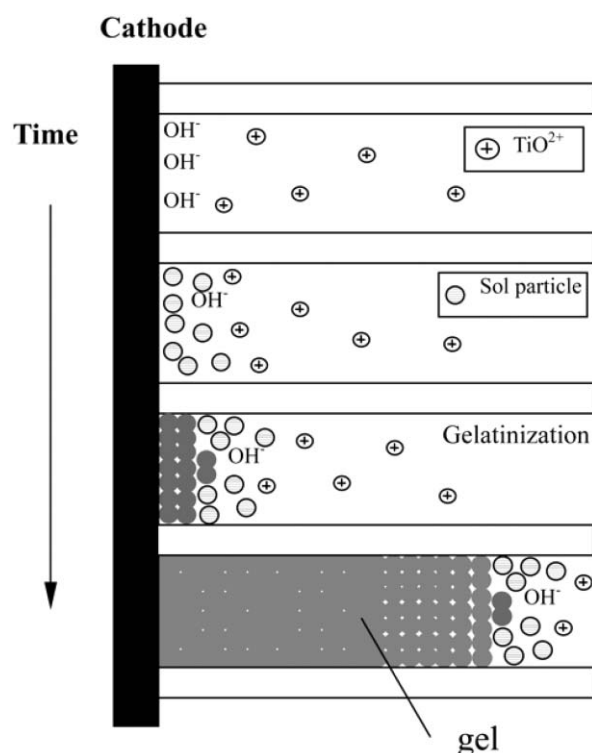
Fig. 1 (A) Scanning electron micrograph (SEM) of 60 nm diameter silica nanotubes. The thickness of the alumina template membrane used was 350 nm, which determines the length of the nanotubes. (B) SEM image of typical alumina membrane. Reprinted with permission from reference 45, © 2002 American Chemical Society.



Scheme 1 Current-time transient for the deposition of 60 nm nickel nanowires into a 6 μm polycarbonate template.

template at high temperatures, causing the wires to crystallize as anatase nanowires.

Martin and co-workers used nanoporous membranes for the



Scheme 2 Schematic illustrating the progress of the electrochemically induced sol-gel process. Xu and co-workers observed both the formation of sol particles and the gelation process in the alumina pores. Reprinted with permission from reference 15, © 2002 American Chemical Society.

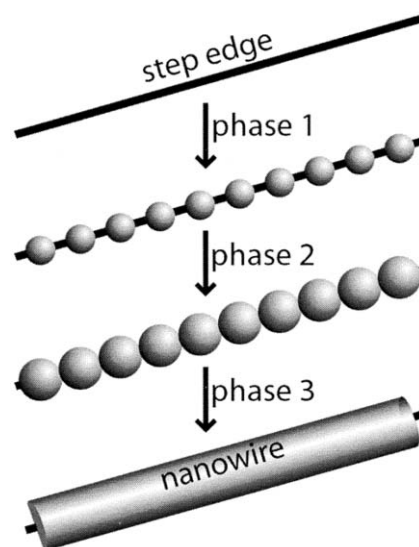
synthesis of nanotubes — hollow versions of the nanowires described above (Fig. 1).^{16,17} For example, silica nanotubes were prepared in alumina templates, using a sol-gel to coat the membrane surfaces.¹⁸ The membrane was immersed in a silica alkoxide solution that coated the membrane faces and the pore walls. With solvent evaporation, SiO_2 nanotubes were formed. The silica on the membrane faces was polished off, and the membrane was dissolved, yielding a nanotube suspension.

Martin and co-workers applied a tin catalyst to the membrane surfaces and pore walls of a polycarbonate nanoporous membrane and then submersed the membrane in an electroless plating solution containing a Au^{I} species and a chemical reducing agent.¹⁹ The reduction of Au^{I} to Au occurred at the catalyst sites on the pore walls and membrane faces, forming gold nanotubes in the pores, as well as gold-coated membrane surfaces. As the reaction time increased, the gold layer grew thicker, and the gold grew from the pore walls inward. Thus, with increased reaction time, the nanotube inner diameter decreased. The membrane was then used as a gold-coated filter. Alternatively, for the isolation of gold nanotubes, the gold membrane surfaces were polished off and the membrane dissolved. If the reaction time was increased, the pores filled completely and nanowires were formed.

Other templated fabrication techniques

Step-edge decoration has been used for the formation of high aspect ratio nanowires along the steps of a crystalline surface (Scheme 3). Common approaches include physical vapor deposition²⁰ or molecular beam epitaxy.²¹ Penner adapted the concept of step-edge formation to the preparation of metallic nanowires *via* electrodeposition on a low energy graphite surface.²² Upon application of a potential, particles of conductive material electrodeposited selectively along the step-edge of the graphite surface. With continued growth, these particles coalesced into nanowires. These nanowires were dimensionally uniform and microns in length. Many varieties of nanowires were synthesized, including MoO_2 , Fe_2O_3 , Cu_2O , Pd, Cu, Au, and Ag.

Surfactant molecules can act as soft templates for the synthesis of nanorods. This is a low-cost method for the chemical formation of copious amounts of small gold nanorods, with dimensions $< 2 \mu\text{m}$. Wang and co-workers reported a surfactant-mediated method for the electrochemical formation of gold nanorods (Fig. 2).²³ El-Sayed and co-workers induced self-assembly of these particles into one-,



Scheme 3 Three phases of nanowire electrodeposition at step edges. Reprinted with permission from reference 22, © 2002 American Chemical Society.

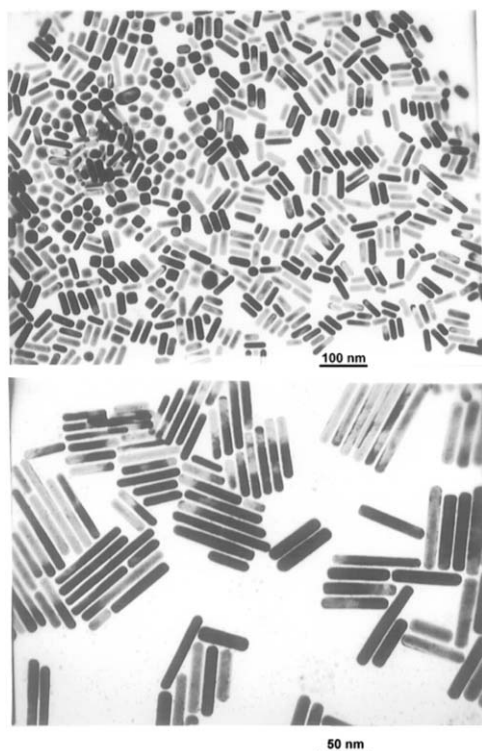


Fig. 2 TEM images of Au nanorods with different mean aspect ratios: 2.6 (top) and 7.6 (bottom). Reprinted with permission from reference 23, © 1997 American Chemical Society.

two-, and three-dimensional arrays.²⁴ Murphy and co-workers increased the yield to over 90% using a chemical reductant.²⁵ The molecular details of how these high aspect ratio particles form is not clear.

Many other methods exist for the solution based synthesis of nanorods. Alivisatos and co-workers have made CdSe in large quantities with variable aspect ratios and excellent monodispersity.^{26,27} They then used CdSe nanorods for the synthesis of CdSe/ZnO core-shell nanorods, varying the shell thickness between one and six monolayers on core nanorods with aspect ratios between 2 : 1 and 10 : 1. Banin and co-workers grew similar structures, growing a ZnS shell onto a CdSe nanorod core through the slow addition of ZnS to a moderate temperature mixture of trioctylphosphine-oxide and hexadecylamine.²⁸

By controlling the water content in the reaction mixture, Pileni and co-workers were able to synthesize metallic copper cylinders through the hydrazine reduction of Cu(AOT)₂.²⁹ Xia and co-workers developed the solution phase synthesis of selenium nanowires with diameters in the range of 10–30 nm.³⁰ The study of solution based synthesis of nanorods and nanowires is quite extensive. Though a few highlights have been discussed, a comprehensive review of this area is not within the scope of this article. For a comprehensive discussion of the chemical synthesis of nanorods, Xia *et al.* have written an excellent review.³¹

High temperature approaches

Carbon nanotubes, synthesized by high temperature processing, are of considerable recent interest. Carbon nanotubes are cylindrical structures consisting of rolled-up graphene sheets with fullerene caps (Fig. 3).³² Carbon nanotubes can be multi-walled, with many concentric cylindrical graphene tubes, or single-walled, with a single cylindrical graphene tube.³³ Carbon nanotubes gained attention for their unique properties, including high tensile strength, high thermal conductivity, and electrical conductivity. They can be metallic or semi-conducting,

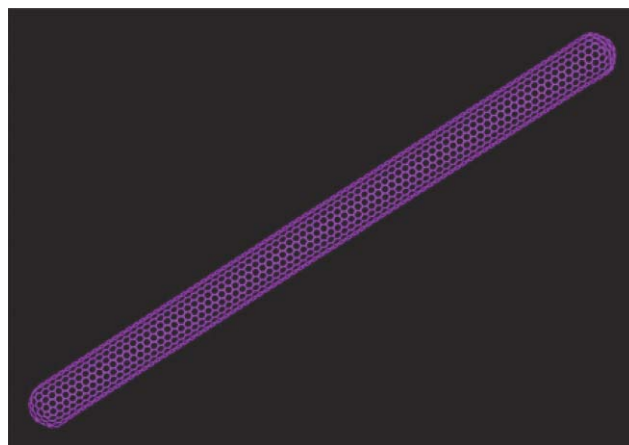


Fig. 3 A single walled carbon nanotube. Taken from ref. 32 with permission.

depending on the nanotube symmetry. Iijima and co-workers first synthesized carbon nanotubes in 1993 *via* the thermal decomposition of hydrocarbons.³³ High temperature decomposition of vapors such as benzene or acetylene, in the presence of Co, Fe, or Ni catalysts, forms single walled carbon nanotubes.³³

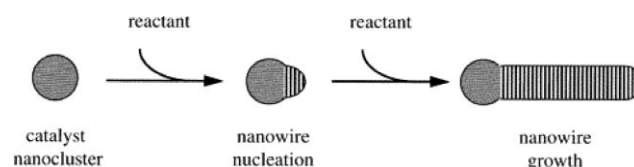
Arc discharge represents an inexpensive way to form carbon nanotubes. An electric arc is generated between two carbon graphite electrodes in a helium atmosphere in the presence of a Fe or Ni catalyst. The carbon nanotubes appear in the form of carbon ash on and around the graphite electrodes. Fischer and co-workers optimized the method to form highly crystalline nanotube bundles at a yield of 70–90%, with nanotube diameters of ~1.4 nm.³⁴

Recently, new methods for the formation of carbon nanotubes have been developed in hopes of increasing nanowire yield and purity. In 1996, Smalley and co-workers developed the laser ablation method for the synthesis of carbon nanotubes.³⁵ This method produces nanotubes spontaneously formed into ropes of 100 to 500 carbon nanotubes, at yields of more than 70%. Avouris and co-workers developed a method for a catalyst-free synthesis of carbon nanotubes on a silicon surface.³⁶ An advantage of this approach is that catalyst removal is not necessary for purification.

Lieber and co-workers developed a catalytic approach for synthesizing single crystal silicon nanowires.³⁷ Nanowire growth results from the site specific precipitation of the silicon on a catalytic nickel–silicon nanocluster (Scheme 4). The wires can be doped with boron or phosphorus to alter the hole or electron density in the silicon, thus making the nanowires p- or n-type semiconductors, respectively.³⁸



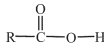
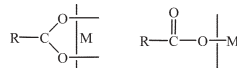
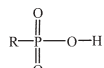
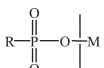
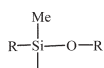
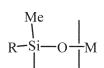
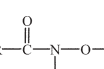
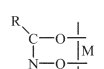
Surface functionalization

Chemical modification of nanowire surfaces is often necessary for nanoparticle functionality and biocompatibility. It is, in fact, essential to many applications covered in this review. At the core of this is a large library of studies on the chemical



Scheme 4 Schematic diagram illustrating the catalytic synthesis of nanowires. Reactant material, which preferentially adsorbed on the catalyst cluster, was added to the growing nanowire at the catalyst–nanowire interface. Reprinted with permission from reference 37, © 1999 American Chemical Society.

Table 2 Ligands and the surfaces they are reported to functionalize

Ligand	Name	Surface modified	Proposed linkage
R-S-H	Thiols	Au, Ag, Cu, Hg, Fe	
R-S-S-R'	Disulfides		
R-C≡N	Isocyanides	Pt, Pd	
	Carboxylic acids	Metal oxides	
	Phosphonates	Metal oxides	
	Siloxanes	Metal oxides	
	Hydroxamic acids	Metal oxides	

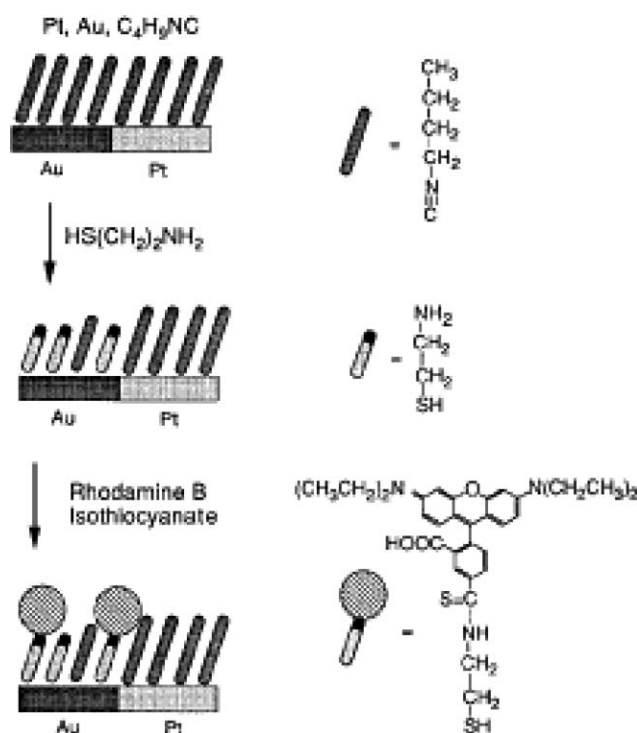
modification of planar surfaces. For example, it is well known that thiols have a high affinity for a gold surface and will often form self-assembled monolayers.³⁹

It is also well known that carboxylic acids and siloxanes will readily bind to a metal oxide surface. Other examples of preferred adsorption of ligands to metal surfaces are given in Table 2.⁴⁰ For example, Wrighton and co-workers reacted a gold surface and a platinum surface with an alkyl thiol and isocyanide.⁴¹ The gold surface selectively bound the thiol and the platinum surface selectively bound the isocyanide. Whitesides and co-workers⁴⁰ used a surface patterned with gold and aluminium stripes to show that a gold surface selectively bound a thiol and an aluminium oxide surface selectively bound a carboxylic acid from the same solution. Examples of studies on the interaction of molecules with high aspect ratio nanoparticles are given below.

Mallouk and co-workers demonstrated functionalization of two-segment metallic nanowires (Scheme 5).^{42,43} A gold-platinum nanowire was reacted with 1-butaneisocyanide and 2-mercaptoethylamine. The expectation was that the isocyanide would bind to the platinum segment while the thiol would bind to the gold segment. Rhodamine B isothiocyanate, which is known to couple with the terminal amine on the gold surface, was reacted with the functionalized nanowires. Fluorescence microscopy showed fluorescent gold segment and a non-fluorescent platinum segment, indicating selective functionalization on the two segments. This fluorescence assay indicated preferential binding of the isocyanide to platinum and the thiol to gold similar to what had been shown on planar surfaces.⁴¹

Meyer and co-workers used a related approach to show orthogonal self-assembly on a two-segment nickel-gold nanowire (Scheme 6).⁴⁴ The nanowires were first reacted with 11-aminoundecanoic acid and 1,9-nonanedithiol. The functionalized wires were then coupled to two different organic dye molecules that preferentially reacted with the thiol and amine groups. The result was a nanowire that emitted light of different colors on each segment, as observed by fluorescence microscopy.

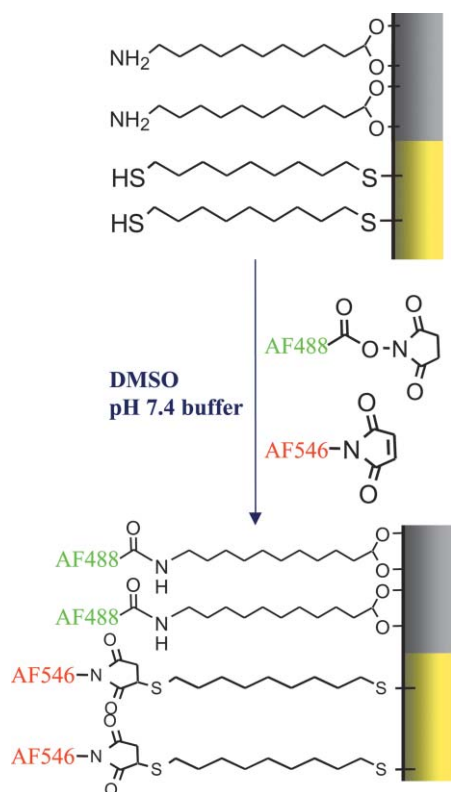
Martin and co-workers functionalized the inside and outside of silica nanotubes with two distinct silane molecules.⁴⁵ Nanotubes in their template were immersed into a silane solution. The silanes attached to the inner surfaces of the nanotube but were prevented from binding to the outer surface



Scheme 5 Functionalization of a two-segment gold-platinum nanowire. Reprinted with permission from reference 42.

by the template. The membrane was then dissolved and the nanotubes were immersed in a second silane solution, which binds to the outer surface of the tube.⁴⁵ A fluorescence assay was used to demonstrate that the desired nanotube functionalization had occurred.

Many techniques exist for carbon nanotube modification for biological applications.⁴⁶ Without modification, carbon nanotubes are insoluble in most solvents. Wong and co-workers modified carbon nanotubes with organic derivatives to increase their solubility in organic and aqueous solvents.⁴⁷ The hydrophobic exterior and hydrophilic core of the crown ether is known to facilitate solubility of large molecules.⁴⁸ When carbon nanotubes were reacted with an amine functionalized crown ether, they became readily soluble in water



Scheme 6 Orthogonal self-assembly on gold and nickel segments of a single nanowire.

(1100 mg L⁻¹) and a variety of organic solvents, including acetone (280 mg L⁻¹) and methanol (1600 mg L⁻¹). Solutions of the functionalized nanotubes were transparent and were characterized by IR and UV-Vis absorption spectroscopies.

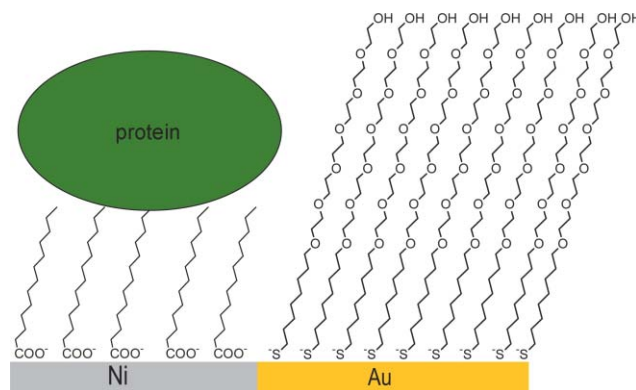
Haller and others studied siloxanes bound to a planar silicon surface as a means to alter the silicon surface properties.⁴⁹ Lieber and co-workers used this approach to modify the silicon oxide surface of silicon nanowires.⁵⁰

Biological modification

Mallouk and co-workers described the use of DNA to assemble gold nanowires.⁵¹ Single-strand DNA (ssDNA) was modified with a thiol at the 5' position and tetramethyl rhodamine at the 3' position. The ssDNA was reacted with gold nanowires. Fluorescence microscopy was used to detect the presence of the attached tetramethyl rhodamine on the surface of the nanowire. ssDNA coated nanowires were then allowed to hybridize with ssDNA coated gold surfaces. Optical micrographs demonstrated that the gold surfaces functionalized with the complementary ssDNA strand had four times as many gold nanowires attached to their surface as did surfaces functionalized with non-complementary ssDNA.

Meyyappan and co-workers developed a method to modify carbon nanotubes that were aligned perpendicular to a planar surface.⁵² The nanotube array was oxidized to introduce carboxylic acid functional groups that were subsequently reacted with amine terminated fluorescent tagged DNA. Evidence for the DNA binding was obtained with a fluorescence microarray scanner. Kappes and co-workers report similar amide coupling of DNA to oxidized carbon nanotube bundles.⁵³ The nanotube-DNA adduct was then reacted with fluorescent labeled complementary or non-complementary ssDNA. Confocal fluorescence imaging showed that the nanotube-DNA adduct selectively hybridizes with complementary strands while minimizing non-specific interactions with non-complementary strands.

It is known that a hexa(ethylene glycol) terminated long

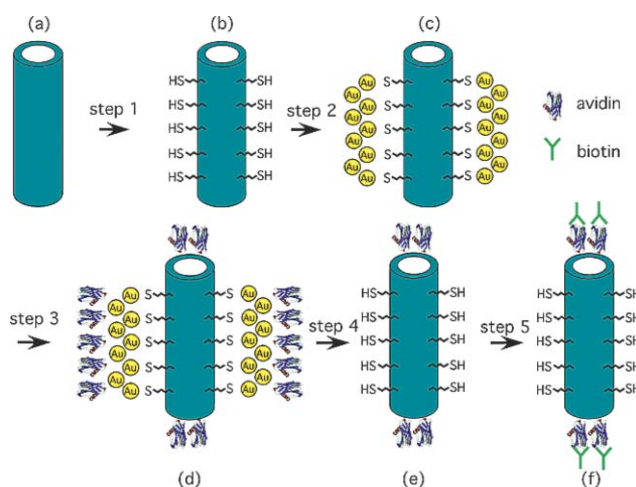


Scheme 7 Selective protein adsorption on a gold-nickel nanowire.

chain thiol covalently bound to a gold surface will resist the non-specific adsorption of protein to that surface.⁵⁴ Meyer and co-workers extended this work to two-segment nickel-gold nanowires that resisted non-specific adsorption of proteins on one segment (Scheme 7).⁵⁵ Nickel-gold nanowires were reacted with palmitic acid and a hexa(ethylene glycol) terminated long chain thiol. These wires were combined with a fluorescent protein that non-specifically adsorbed to the hydrophobic nickel nanowire segment. However, the gold nanowire segment, with the hydrophilic ethylene glycol coating, resisted protein adsorption. Fluorescence microscopy was again used to observe the fluorescent protein preferentially absorbed to the nickel segment of the nanowire.

The protein avidin is known to non-specifically bind to most materials, including carbon nanotubes. Matsui and co-workers used selective etching to prevent non-specific avidin binding (Scheme 8).⁵⁶ The sides of the carbon nanotubes were coated with a gold nanocrystal mask and were then reacted with avidin. Avidin adsorbed non-selectively to the nanotube ends and the gold nanocrystal mask, but was prevented from binding to the nanotube sides. The gold nanocrystals were etched and only the nanowire ends were covered in avidin, as shown by fluorescence microscopy. These end-functionalized avidin wires were then directed to complementary biotin labeled surfaces as a means toward nanotube immobilization.⁵⁶

As another means to prevent protein binding, Dai and co-workers reported the surfactant-aided adsorption of poly(ethylene glycol) to a carbon nanotube. The poly(ethylene glycol) coated nanotube resisted non-specific absorption by streptavidin.⁵⁷



Scheme 8 Procedure to immobilize proteins at the ends of nanotubes using nanocrystals as protective masks. Reprinted with permission from reference 56, © 2003 American Chemical Society.

III. Applications

Separations

A common application of high aspect ratio nanoparticles is for separation and isolation of a specific analyte from complex mixtures. There are several recent examples from the group of C. R. Martin of nanotubes being used as selective filters for proteins and other biologically important molecules. These nanotubes were all fabricated using nanoporous membranes as a template. In the first example, silica nanotubes were synthesized in an alumina membrane using a sol-gel method.⁴⁵ They were functionalized with octadecyl silane on the inside, resulting in a hydrophobic nanotube interior, while the outside was left unfunctionalized, giving hydrophilic surface chemistry on the exterior of the nanotubes. These hydrophobic/hydrophilic nanotubes were successfully used for extracting lipophilic compounds from aqueous solution. The tubes were added to an aqueous solution of 7,8-benzoquinoline, a lipophilic compound that preferentially entered the hydrophobic interior of the nanotubes. In this way, more than 90% of the compound was removed from the solution.

Martin and co-workers have also shown that enantiomers of a drug can be separated using a suspension of nanotubes.⁴⁵ In this case, the nanotubes were functionalized with an aldehyde-terminated silane, which was coupled to an antibody that specifically binds the *RS* isomer of the drug 4-[3-(4-fluorophenyl)-2-hydroxy-1-[1,2,4]-triazol-1-yl-propyl]-benzonitrile (FTB) over the *SR* isomer. These nanotubes successfully extracted 75% of the *RS* isomer from a 20 μ M racemic mixture, and all of the *RS* isomer from a 10 μ M racemic mixture.

In the next examples, Martin and co-workers did not remove the nanoparticles from the templates. This resulted in a membrane with embedded nanotubes, which was used to study selective transport of biological molecules.^{58,59} First, the size-selective transport of proteins using gold nanotubes inside a polycarbonate membrane was studied.⁵⁸ The interior of these tubes was functionalized with thiol-terminated poly(ethylene glycol) (PEG). These functionalized nanotube membranes were placed in solutions of proteins such as lysozyme and bovine serum albumen (BSA) and the flux of protein through the membrane was monitored by high pressure liquid chromatography. For gold nanotube membranes with an inner diameter of 23 nm, plots of moles of lysozyme transported vs. time were linear for up to five days. However, in nanotubes that were not modified with PEG, the transport of lysozyme stopped after about eight hours (Fig. 4). This indicated that the non-PEGylated nanotubes were quickly blocked by adsorbed

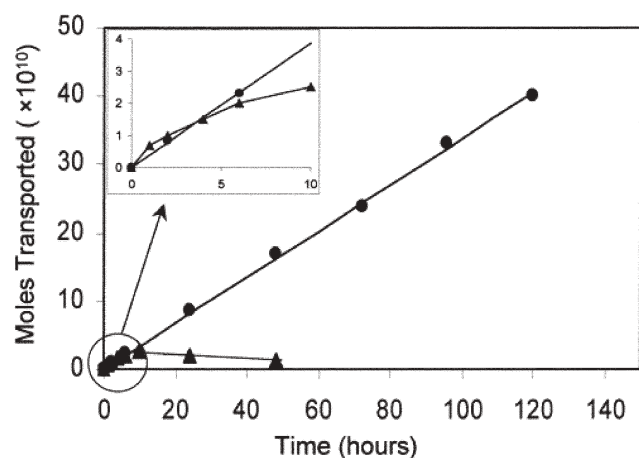


Fig. 4 Moles transported vs. time across a 23 nm Au nanotube membranes. Upper line: with chemisorbed PEG-thiol. Lower curve: no PEG thiol. The inset shows the initial transport rates of lysozyme. Reprinted with permission from reference 58, © 2001 American Chemical Society.

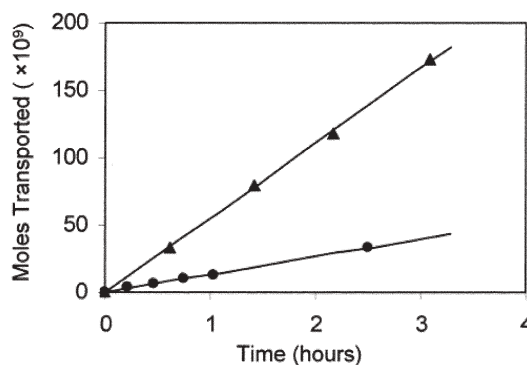


Fig. 5 Plots of moles transported vs. time for lysozyme (upper) and BSA (lower) across a 40 nm Au nanotube membrane. Reprinted with permission from reference 58, © 2001 American Chemical Society.

protein, while the PEG functionalization clearly prevented such blockage. A comparison of the flux of two different proteins was also carried out. It was shown that in 40 nm tubes, the flux of lysozyme was four times greater than that of BSA, even though lysozyme is only 1.8 times smaller than BSA, indicating a hindered transport mechanism (Fig. 5).⁶⁰ This difference in flux was exploited for separating a mixture of the two proteins. Martin and co-workers found that the selectivity of separating BSA and lysozyme increased as nanotube inner diameter decreased, demonstrating that the separation is size-based. They concluded that although the membrane porosities were too low for practical use in protein separation, the nanotube membranes might be useful for future sensor applications.

In a more recent paper,⁵⁹ Martin and co-workers again looked at the separation of the *RS* and *SR* enantiomers of FTB, as described above. In this case, a silica nanotube membrane was modified with the antibody that selectively binds the *RS* isomer. They found that these membranes facilitate the transport of the *RS* isomer, as the *RS* flux was twice the *SR* flux. This selective transport of one enantiomer over the other resulted in the separation of the two drug isomers. It was also shown that the binding affinity of *RS* over *SR* could be tuned by addition of DMSO to the protein buffer solution, leading to an optimal DMSO content that maximized the selectivity. The selectivity could be further enhanced by decreasing the pore size and thus shutting down non-facilitated transport (*i.e.*, diffusion) of the unwanted enantiomer. However, this had the unwanted effect of slowing down the flux as well.

The use of nanotubes for selective separation of biological molecules seems like a logical step given the average dimensions of the particles and their origin inside nanoporous filter membranes. However, there are other classes of materials that have also demonstrated their usefulness in separations technology. Magnetic nanoparticles are now in widespread use in cell separation.⁶¹ Currently, magnetic beads are the most common commercially available nanoparticle for magnetic cell separations. These beads often contain small iron oxide particles embedded in a spherical polymer matrix.^{1,2} A recent study by Reich and co-workers demonstrated the utility of high aspect ratio magnetic nanowires for cell manipulation and contrasted these results with commercially available magnetic beads.⁶² The nanowires were synthesized by electrodeposition of nickel into nanoporous alumina membranes and isolated as a suspension. Nickel is a ferromagnetic material, meaning the nickel nanowires retain some magnetization even when outside of a magnetic field. Reich and co-workers introduced suspensions of nickel wires or of magnetic beads to cultures of NIH 3T3 cells. They found that the magnetic particles attached to the cells, and they studied the efficiency of separating cells with bound particles from those without.

They showed that the magnetic nanowires outperformed magnetic beads of the same volume by about a factor of two. The yield of isolated cells was $49 \pm 3\%$ for nickel nanowires compared to $19 \pm 2\%$ for the beads. This increase in efficiency was attributed to the higher magnetic moment of the nanowires compared to the beads, a result of the nanowires' large aspect ratio.

Glucose sensing

A second common biological application of high aspect ratio nanoparticles is in sensing. Glucose has emerged as a popular substrate for biosensing applications because of its importance in the healthcare field. In the next section, several methods of glucose sensing using high aspect ratio nanoparticles will be presented, beginning with carbon nanotube-based sensors. Due to their unique electronic properties, carbon nanotubes have recently attracted much attention in the area of sensing.⁶³

Davis and co-workers have studied the amperometric sensing ability of single-walled carbon nanotubes (SWNTs) with non-covalently bound enzymes.⁶⁴ SWNTs with adsorbed glucose oxidase (GOx) were drop-dried onto glassy carbon and used as electrodes in solutions of interest. In the presence of glucose, large anodic current responses were observed at these electrodes, consistent with catalytic oxidation of glucose. This demonstrates that enzymatic activity was not lost upon immobilization to the carbon nanotubes. The current in this experiment was more than ten times greater than that observed at the same electrode with immobilized GOx but without the SWNTs. This is attributable not only to the high enzyme loading on the nanotubes, but also to their high conductance and transducing ability.

Since 1998,⁶⁵ scientists have been exploring the possibility of using individual semiconducting SWNTs as sensors by incorporating them into field-effect transistors (FETs). An FET consists of two electrodes, a source and a drain, connected by a semiconducting channel. Current can only flow through the semiconductor when the appropriate voltage is applied to a third electrode, the gate. Dekker and co-workers were the first to report a single nanotube biosensor to detect glucose.⁶⁶ They fabricated SWNTs by chemical vapor deposition and attached a lithographically patterned electrode to each end. GOx was immobilized onto the tube using pyrene butanoic acid as a coupling agent, where the pyrene binds to the nanotube through van der Waals interactions and the carboxylic acid forms an amide bond with the enzyme. Fig. 6 shows an idealized schematic picture of the nanotube setup. Dekker and co-workers found that only 50 or 60 GOx molecules were sufficient to significantly change the nanotube capacitance. Upon glucose addition, an increase in conductance was observed, indicating a response to the enzyme activity. This change in conductance demonstrates that a glucose sensor can be constructed from an individual SWNT.

Another recent publication involving carbon nanotubes for glucose sensing takes a different approach. In this work, Wang and co-workers made composite electrodes by mixing carbon nanotubes with granular Teflon.⁶⁷ In this arrangement, the carbon nanotubes are the conductive component and the

Teflon acts as a binder. Analogous systems using graphite/Teflon composites have been extensively studied.⁶⁸ Using the carbon nanotube/Teflon composites, H_2O_2 and NADH redox activity was observed at potentials significantly lower than can be observed at graphite/Teflon electrodes. This low-potential detection of H_2O_2 and NADH makes the carbon nanotube/Teflon composite electrode attractive for biosensing if used in conjunction with oxidase and dehydrogenase enzymes. Wang and co-workers accomplished this by incorporating either GOx or alcohol dehydrogenase in the composite, so that the bulk of the electrode acted as a reservoir for the enzyme. Using these electrodes, they carried out amperometric sensing of glucose and ethanol and large signals were observed. Because of the low-potential detection, these carbon nanotube/Teflon composite electrodes were also quite selective; they showed no response to common interferences such as acetaminophen or uric acid. The composite nature of these electrodes is attractive because it combines the electronic properties of carbon nanotubes with the advantages of bulk electrodes.

Amperometric glucose sensing has also been carried out using vertically aligned arrays of high aspect ratio nanoparticles. This includes arrays of carbon nanotubes coated with a polymer film in which glucose oxidase was entrapped,⁶⁹ as well as electrolessly deposited gold nanotubes with covalently bound GOx.⁷⁰ In the latter case, a current response of $400 \text{ nA mM}^{-1} \text{ cm}^{-2}$ was observed, which is among the highest reported in the literature. Arrays of carbon nanotubes have also been used to detect subattomole amounts of DNA.⁷¹

Protein sensing

In addition to glucose sensing, several groups have become interested in using high aspect ratio nanoparticles for detecting proteins. The extremely strong non-covalent interaction between biotin and streptavidin is often exploited for developing protein recognition devices. Lieber and co-workers have demonstrated that 10 pM concentrations of streptavidin can be detected using a silicon nanowire FET.⁷² These semiconducting nanowires were functionalized with biotin, a ligand that binds to the streptavidin protein with a binding constant of approximately 10^{15} .⁷² An increase in conductance of the biotin-modified silicon nanowire was observed upon addition of streptavidin. Control experiments showed no non-specific binding of streptavidin to the nanowire, indicating that the increase in conductance is caused by the specific biotin-streptavidin interaction. Since the biotin-streptavidin binding is essentially irreversible, Lieber and co-workers also studied the reversible binding of biotin and monoclonal antibiotin. They were able to observe the binding and dissociation in real time. They monitored the nanowire conductance as a function of antibiotin concentration and a linear response was observed. This is an important proof-of-concept for nanowire-based biosensing. By binding the appropriate agents to the silicon nanowire, Lieber and co-workers also made pH and Ca^{2+} sensors.⁷²

In a more recent paper, Star and co-workers detected biotin-streptavidin binding using a carbon nanotube-based FET.⁷³ In this case, the nanotube was coated with a mixture of poly(ethylene glycol) and poly(ethylene amine). The nanotube was biotinylated by amide bond formation with the primary amine groups, while the poly(ethylene glycol) served to prevent protein adsorption to the nanotube. Upon exposure of this device to streptavidin, a loss of current was observed at negative gate voltages. This again demonstrates protein recognition by a nanoscale sensor.

Gene delivery

A final application of high aspect ratio nanoparticles is as a delivery vector. Leong and co-workers have recently

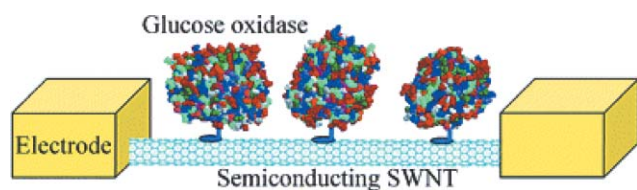


Fig. 6 Schematic picture of two electrodes connecting a semiconducting nanotube with glucose oxidase immobilized on its surface. Reprinted with permission from reference 66, © 2003 American Chemical Society.

demonstrated the use of multifunctional nanorods for gene delivery.⁷⁴ They fabricated nickel–gold nanorods by templated electrodeposition in alumina membranes. Transferrin, an iron transport protein, was bound to the gold segment through a thiol linkage. This served to promote cellular uptake of the particles by a receptor-mediated pathway. The nickel portion of the nanorods was functionalized with 3-[2-(aminoethyl)-dithio]propionic acid. DNA plasmids which encoded a fluorescent reporter gene were electrostatically bound to the terminal amines, while the central disulfide bond served as a cleavable group to release the DNA. *In vitro* transfection studies of these functionalized nanorods were carried out using the Human Embryonic Kidney 293 cell line. Results from both SEM and confocal microscopy indicated that the nanorods were internalized by the cells, although they did not enter the nucleus. However, green fluorescence was observed, indicating delivery of the reporter gene to the nucleus. Overall, these bifunctional nanorods provided good transfection efficiency, and preliminary *in vivo* studies have indicated potential for genetic vaccination applications. The selective surface chemistry of these bifunctional nanorods enabled the attachment of two different spatially segregated functionalities — one to target the cell and the other to deliver the DNA.

IV. Conclusion

In conclusion, we have described the synthesis of a wide variety of high aspect ratio nanoparticles that have recently been reported in the literature. The inherent chemical, optical, magnetic, or electronic properties of the particles can be exploited for new applications in biology that are not possible with the more common and traditional spherical particles. Indeed, reports have already appeared describing the use of high aspect ratio nanoparticles for biological sensing, separations, and gene delivery. The discovery of single nanoparticle FETs could revolutionize the area of sensing, leading to extremely low limits of detection. Separations technology might be greatly enhanced by the development of chemically modifiable nanotube membranes that can be tailored to selectively interact with molecules of interest. Other areas of science could also be improved by the integration of high aspect ratio nanoparticles in biology in ways not yet discovered. The number of literature reports is rapidly increasing and the future of biological applications of high aspect ratio nanoparticles promises to be even more exciting.

V. Acknowledgements

The authors acknowledge equipment support from the NSF MRSEC Grant number DMR00-80031. The authors acknowledge support from DARPA/AFOSR Grant F49620-02-1-0307 and from The David and Lucille Packard Foundation Grant #2001-17715.

VI. References

- 1 Polysciences, Inc. www.polysciences.com.
- 2 Dynal Biotech. www.dynalbiotech.com.
- 3 B. Dubertret, P. Skourides, D. J. Norris, V. Noireaux, A. H. Brivanlou and A. Libchaber, *Science*, 2002, **298**, 1759.
- 4 BioRad Helios Gene Gun. www.biorad.com.
- 5 G. E. Possin, *Rev. Sci. Instrum.*, 1970, **41**, 772.
- 6 J. Choi, M. Neilsch, M. Reiche, R. B. Wehrspoon and U. Gosele, *J. Vac. Sci. Technol., B*, 2003, **35**, 1097.
- 7 Whatman, Inc. www.whatman.com.
- 8 L. Sun, C. L. Chien and P. C. Searson, *J. Mater. Sci.*, 2000, **35**, 1097.
- 9 T. M. Whitney, J. S. Jiang, P. C. Searson and C. L. Chien, *Science*, 1993, **261**, 1316.
- 10 C. R. Martin, *Chem. Mater.*, 1996, **8**, 1739.
- 11 R. M. Penner and C. R. Martin, *Anal. Chem.*, 1987, **59**, 2625.
- 12 C. R. Martin, *Science*, 1994, **266**, 1961.
- 13 Y. Li, G. W. Meng, L. D. Zhang and F. Philipp, *Appl. Phys. Lett.*, 2000, **76**, 2011.
- 14 S. R. Nicewarmer-Pena, R. G. Freeman, B. R. Reiss, L. He, I. D. Walton, R. Cromer, C. D. Keating and M. J. Natan, *Science*, 2001, **294**, 137.
- 15 Z. Maio, D. Xu, J. Ouyang, G. Guo, X. Zhao and Y. Tang, *Nano Lett.*, 2002, **2**, 717.
- 16 M. Nishizawa, V. P. Menon and C. R. Martin, *Science*, 1995, **268**, 700.
- 17 M. Wirtz and C. R. Martin, *Adv. Mater.*, 2003, **15**, 455.
- 18 E. D. Steinle, D. T. Mitchell, M. Wirtz, S. B. Lee, V. Y. Young and C. R. Martin, *Anal. Chem.*, 2002, **74**, 2416.
- 19 V. P. Menon and C. R. Martin, *Anal. Chem.*, 1995, **67**, 1920.
- 20 D. Y. Petrovich, F. J. Himpel and T. Jung, *Surf. Sci.*, 1998, **417**, 189.
- 21 A. Sugawara, T. Coyle, G. G. Hembree and M. R. Scheinfein, *Appl. Phys. Lett.*, 1997, **70**, 1043.
- 22 R. M. Penner, *J. Phys. Chem. B*, 2002, **106**, 3339.
- 23 Y.-Y. Yu, S.-S. Chang, C.-L. Lee and C. R. C. Wang, *J. Phys. Chem. B*, 1997, **101**, 6661.
- 24 B. Nikoobakht, Z. L. Wang and M. A. El-Sayed, *J. Phys. Chem. B*, 2000, **104**, 8635.
- 25 B. D. Busbee, S. O. Obare and C. J. Murphy, *Adv. Mater.*, 2003, **15**, 414.
- 26 J. Hu, L.-S. Li, W. Yang, L. Manna, L.-W. Wang and A. P. Alivisatos, *Science*, 2001, **292**, 2060.
- 27 X. Peng, *Nature*, 2000, **404**, 59.
- 28 T. Mokari and U. Banin, *Chem. Mater.*, 2003, **15**, 3955.
- 29 J. Tanori and M. P. Pileni, *Langmuir*, 1997, **13**, 639.
- 30 B. Gates, Y. Yin and Y. Xia, *J. Am. Chem. Soc.*, 2000, **122**, 12582.
- 31 Y. Xia, P. Yang, Y. Sun, Y. Wu, B. Mayers, B. Gates, Y. Yin, F. Kim and H. Yan, *Adv. Mater.*, 2003, **15**(15), 353.
- 32 Carbon Nanotechnologies Web Site, www.cnanotech.com.
- 33 S. Iijima and T. Ichihashi, *Nature*, 1993, **363**, 603.
- 34 C. Journet, W. K. Maser, P. Bernier, A. Loiseau, M. Lamy de la Chapelle, S. Lefrant, P. Denierd, R. Lee and J. E. Fischer, *Nature*, 1997, **388**, 756.
- 35 A. Thess, R. Lee, P. Nikolaev, H. Dai, P. Petit, J. Robert, C. Xu, Y. H. Lee, S. G. Kim, A. G. Rinzler, D. T. Colbert, G. E. Scuseria, D. Tomanek, J. E. Fischer and R. E. Smalley, *Science*, 1996, **273**, 483.
- 36 V. Derycke, R. Martel, M. Radosavljevic, F. M. Ross and Ph. Avouris, *Nano Lett.*, 2002, **2**, 1043.
- 37 J. Hu, T. W. Odom and C. M. Lieber, *Acc. Chem. Res.*, 1999, **32**, 435.
- 38 Y. Cui, X. Duan, J. Hu and C. M. Lieber, *J. Phys. Chem. B*, 2000, **104**, 5213.
- 39 C. D. Bain, E. B. Troughton, Y.-T. Tao, J. Evall, G. M. Whitesides and R. G. Nuzzo, *J. Am. Chem. Soc.*, 1989, **111**, 321.
- 40 P. E. Laibinis, J. J. Hickman, M. S. Wrighton and G. M. Whitesides, *Science*, 1989, **245**, 845.
- 41 J. J. Hickman, P. E. Laibinis, D. I. Auerbach, C. Zou, T. J. Gardner, G. M. Whitesides and M. S. Wrighton, *Langmuir*, 1992, **8**, 357.
- 42 B. R. Martin, D. J. Dermody, B. R. Reiss, M. Fang, L. A. Lyon, M. J. Natan and T. E. Mallouk, *Adv. Mater.*, 1999, **11**, 1021.
- 43 N. I. Kovtyukhova and T. E. Mallouk, *Chem. Eur. J.*, 2002, **8**, 4354.
- 44 L. A. Bauer, D. H. Reich and G. J. Meyer, *Langmuir*, 2003, **19**, 7043.
- 45 D. T. Mitchell, S. B. Lee, L. Trofin, N. Li, T. K. Nevanen, H. Soderlund and C. R. Martin, *J. Am. Chem. Soc.*, 2002, **124**, 11864.
- 46 Y.-P. Sun, K. Fu, Y. Lin and W. Huang, *Acc. Chem. Res.*, 2002, **35**, 1096.
- 47 M. G. C. Kahn, S. Banerjee and S. S. Wong, *Nano Lett.*, 2002, **2**, 1215.
- 48 C. J. Pederson, *J. Am. Chem. Soc.*, 1967, **89**, 7017.
- 49 I. Haller, *J. Am. Chem. Soc.*, 1978, **100**, 8050.
- 50 Y. Cui, Q. Wei, H. Park and C. M. Lieber, *Science*, 2001, **293**, 1289.
- 51 J. K. Mbindyo, B. D. Reiss, B. R. Martin, C. D. Keating, M. J. Natan and T. E. Mallouk, *Adv. Mater.*, 2001, **13**, 249.
- 52 C. V. Nguyen, L. Delzeit, A. M. Cassell, J. Li, J. Han and M. Meyyappan, *Nano Lett.*, 2002, **2**, 1079.
- 53 M. Hazani, R. Neeman, F. Hennrich and M. M. Kappes, *Nano Lett.*, 2003, **3**, 153.
- 54 K. L. Prime and G. M. Whitesides, *Science*, 1991, **252**, 1164.
- 55 N. S. Birenbaum, T. B. Lai, D. H. Reich, C. S. Chen and G. J. Meyer, *Langmuir*, 2003, **19**, 9580.

- 56 I. A. Banerjee, L. Yu and H. Matsui, *Nano Lett.*, 2003, **3**, 283.
- 57 M. Shim, N. W. S. Kam, R. J. Chen, Y. Li and H. Dai, *Nano Lett.*, 2002, **2**, 285.
- 58 S. Yu, S. B. Lee, M. Kang and C. R. Martin, *Nano Lett.*, 2001, **1**, 495.
- 59 S. B. Lee, D. T. Mitchell, L. Trofin, T. K. Nevanen, H. Söderlund and C. R. Martin, *Science*, 2002, **296**, 2198.
- 60 C. R. Martin, M. Nishizawa, K. Jirage and M. Kang, *J. Phys. Chem. B*, 2001, **105**, 1925.
- 61 Q. A. Pankhurst, J. Connolly, S. K. Jones and J. Dobson, *J. Phys. D: Appl. Phys.*, 2003, **36**, R167.
- 62 A. Hultgren, M. Tanase, C. S. Chen, G. J. Meyer and D. H. Reich, *J. Appl. Phys.*, 2003, **93**, 7554.
- 63 Q. Zhao, Z. Gan and Q. Zhuang, *Electroanalysis (N. Y.)*, 2002, **14**, 1609.
- 64 B. R. Azamian, J. J. Davis, K. S. Coleman, C. B. Bagshaw and M. L. H. Green, *J. Am. Chem. Soc.*, 2002, **124**, 12664.
- 65 S. J. Tans, A. R. M. Verschueren and C. Dekker, *Nature*, 1998, **393**, 49.
- 66 K. Besteman, J. Lee, F. G. M. Wiertz, H. A. Heering and C. Dekker, *Nano Lett.*, 2003, **3**, 727.
- 67 J. Wang and M. Musameh, *Anal. Chem.*, 2003, **75**, 2075.
- 68 N. Peña, G. Ruiz, J. Reviejo and J. M. Pingarrón, *Anal. Chem.*, 2001, **73**, 1190–1195.
- 69 M. Gao and G. G. Wallace, *Synth. Met.*, 2003, **137**, 1393.
- 70 M. Delvaux and S. Demoustier-Champagne, *Biosens. Bioelectron.*, 2003, **18**, 943.
- 71 J. Li, H. T. Ng, A. Cassell, W. Fan, H. Chen, Q. Ye, J. Loehne, J. Han and M. Meyyappan, *Nano Lett.*, 2003, **3**, 597.
- 72 Y. Cui, Q. Wei, H. Park and C. M. Lieber, *Science*, 2001, **293**, 1289.
- 73 A. Star, J.-C. P. Gabriel, K. Bradley and G. Grüner, *Nano Lett.*, 2003, **3**, 459.
- 74 A. K. Salem, P. C. Searson and K. W. Leong, *Nature Mater.*, 2003, **2**, 668.